Pion elastic and inelastic scattering on s-d shell nuclei in the Δ_{33}-resonance region. Coupled-channel analysis

M. Gmitro* and J. Kvasil†
Laboratory of Theoretical Physics, JINR, Dubna, SU 101 000, Moscow, USSR

R. Mach
Institute of Nuclear Physics, ČSAV, CS 25068, Řež, Czechoslovakia

(Received 28 June 1984)

Equations of the coupled-channel method are solved in momentum space for pion scattering on ^{24,26}Mg and ^{28}Si in the Δ_{33}-resonance region. The elastic and inelastic differential cross sections are calculated by using the nuclear ground-state and transition densities which correctly describe the (e,e′) data for the same nuclear states. Also calculated are the double-analog double-charge-exchange reactions ^{26}Mg$(\pi^+,\pi^-)^{26}$Si and ^{18}O$(\pi^+,\pi^-)^{18}$Ne, and the results obtained are in surprisingly good agreement with the experimental data. From the comparison of our coupled-channel and distorted-wave impulse approximation results we conclude that the multistep mechanisms play a minor role in the reactions considered.

I. INTRODUCTION

In recent years, the number of precise measurements of pion inelastic scattering to definite excited nuclear states for a variety of nuclear targets has increased. Most of such reactions seem to have a one-step character, i.e., DWIA calculations reproduce the gross features of differential cross sections satisfactorily. Such calculations were done, e.g., by Lee and Kurath[1] for a variety of p-shell nuclei. The most ambitious DWIA-type calculations up to now were performed by Lenz *et al.*[2] using the isobar-doorway model. They took into account the modifications of the elementary πN amplitude in the nuclear medium as well as the pion annihilation effects (at least at the phenomenological level). These modifications give a considerable contribution in some kinematical situations. Generally a small effect of multistep mechanisms was expected also in some earlier papers (see, e.g., Ref. 34).

On the other hand, it is well known that not all inelastic processes can be accounted for by DWIA-type calculations. A well-known example is the charge-exchange reaction ^{13}C$(\pi^+,\pi^0)^{13}$N. Here, the coupled-channel calculations[3] remove, to some extent, the long-standing discrepancy between DWIA results and the experiment. There are also other inelastic transitions[4] where the multistep processes seem to play a vital role.

The aim of the present paper is to develop a workable formalism for coupled-channel calculations of pion elastic and inelastic scattering processes. The method is based on the multiple-scattering theory and enables one to take into account simultaneously a rather large number of nuclear excited states (up to ten or so) and to investigate in this way the multistep aspects of the pion-nucleus reactions.

Such aspects are of special interest in the pion scattering by deformed sd-shell nuclei. In proton scattering by such nuclei, excited states are strongly populated and play an important part in any description of proton scattering processes.[5] It is quite possible that the collective low-lying excited states may make the multistep pion processes also rather strong for this group of nuclei. The failure of the Glauber model calculations in describing the pion inelastic scattering in ^{24}Mg seems to support this point of view.[6]

In the work reported in the present paper, detailed calculations have been performed for pion elastic and inelastic scattering on ^{24,26}Mg and ^{28}Si in the Δ_{33}-resonance region, where there exist high-quality experimental data. We study also the double-analog double-charge exchange (DCE) reaction ^{26}Mg$(\pi^+,\pi^-)^{26}$Si, which provides a rather stringent test of the model developed. The comparison is made with the similar DCE reaction ^{18}O$(\pi^+,\pi^-)^{18}$Ne. The two DCE reactions were rather extensively investigated on the basis of the Glauber model with mesonic exchange-current contributions,[7] and the optical models with the second-order pion-nucleus interaction,[8] and using the isobar dynamics.[35]

The coupled-channel calculations are compared here with the DWIA results obtained under the same kinematical and dynamical assumptions in constructing the corresponding transition matrix elements. Such a comparison reveals the role of channel coupling in the transitions studied. We also performed several calculations assuming the pion on-energy-shell propagation through the nucleus. An estimation of the off-energy-shell effects was obtained in this way for the reaction under consideration.

The paper is organized as follows. The coupled-channel formalism is briefly developed in Sec. II. The procedure for obtaining the nuclear densities from the electron scattering experiments is described in Sec. III. Our calculated results are presented and compared with the experimental data in Sec. IV. The conclusions are given in Sec. V.

II. COUPLED-CHANNEL FORMALISM

We start with multiple scattering theory,[9] in the framework of which the pion-nucleus scattering matrix $T(E)$ can be written in terms of the auxiliary matrix

$$T'(E)=(A-1)T(E)/A$$

as

$$T'(E)=(A-1)\tau(E)[1+G(E)T'(E)]\ , \tag{2.1}$$

where the Green's function

$$G(E)=(E-K_\pi-H_A+i\epsilon)^{-1}$$

contains the nuclear Hamiltonian H_A and the pion kinetic energy operator K_π. Furthermore,

$$\tau(E)=v+v\mathscr{A}G(E)\tau(E) \tag{2.2}$$

is the pion-bound nucleon scattering matrix, v denotes the pion-nucleon potential, and A is the number of nucleons.

Two projection operators P_0 and Q_0 are defined as

$$P_0=\sum_{n\in P}|n\rangle\langle n|\ ,\quad Q_0=\sum_{n\notin P}|n\rangle\langle n|\ ,\quad P_0+Q_0=\mathscr{A}\ , \tag{2.3}$$

the first of which projects onto the nuclear states that are explicitly taken into account (P space), whereas Q_0 projects onto the remaining states. Equation (2.1) takes the form

$$T'(E)=U(E)[1+P_0G(E)T'(E)]\ , \tag{2.4}$$

where the potential matrix is given by

$$U(E)=(A-1)\tau(E)[1+Q_0G(E)U(E)]\ . \tag{2.5}$$

Neglecting the nuclear excitations out of the P space, we have

$$U(E)\simeq(A-1)\tau(E) \tag{2.6}$$

and

$$\langle m|T'(E)|0\rangle=(A-1)\sum_{n\in P}\langle m|\tau(E)|n\rangle[\delta_{n0}+G_{nn}(E)\langle n|T'(E)|0\rangle]\ , \tag{2.7}$$

where $G_{nn}(E)=\langle n|G(E)|n\rangle$.

A. Impulse approximation

Since $\tau(E)$ is a complicated $(A+1)$-body quantity, we approximate it by the much more simple three-body operator[10]

$$T_{\pi A}(E)=v+vd(E)T_{\pi A}(E)\ , \tag{2.8}$$

where

$$d(E)=(E-K_\pi-k_1-k_C-U_C+i\epsilon)^{-1}\ . \tag{2.9}$$

Here, k_1 and k_C are the kinetic energy operators of the target nucleon and of an $(A-1)$-nucleon core, respectively. The constant $U_C<0$ is chosen to have approximately the magnitude of the nucleon-core potential energy.

The relation

$$\tau(E)=T_{\pi A}(E)+T_{\pi A}(E)[\mathscr{A}G(E)-d(E)]\tau(E) \tag{2.10}$$

holds and the impulse approximation consists of $\tau(E)\simeq T_{\pi A}(E)$. Since the approximation is based on the pion-nucleon-core kinematics [see Eq. (2.9)], it is usually called the "three-body" model. The model leads to a Galilean-invariant potential matrix[11]

$$U(E)=(A-1)T_{\pi A}(E)\ , \tag{2.11}$$

and was successfully applied by Landau and Thomas[10] in studying the pion elastic scattering by the helium isotopes.

A question arises whether our step beyond the coherent scattering approximation (introducing a larger model space P than just $P^{(0)}=|0\rangle\langle 0|$) should not be accompanied by a corresponding modification of the impulse approximation, since the corrections to the coherent scattering approximation (CSA) and the impulse approximation (IA) tend to cancel each other to some extent.[12] Such a modification of the IA is technically rather involved. Moreover, Kerman, McManus, and Thaler[9] have shown that at least for small transferred momenta, the corrections to the IA are roughly A times as small as those to the CSA. Therefore, we expect that our model [i.e., Eqs. (2.7) and (2.11)] represents a reasonable approximation except for the very light ($A\lesssim 10$) nuclei.

B. Elements of the potential matrix

Prior to the derivation of the potential matrix $U(E)$, we recall the obvious identity

$$\begin{aligned}&\langle\vec{p}\,',\vec{k}\,'_1,\vec{k}\,'_C|T_{\pi A}(E)|\vec{k}_C,\vec{k}_1,\vec{p}\rangle\\&\quad=(2\pi)^6\delta^{(3)}(\vec{p}\,'+\vec{k}\,'_1-\vec{p}-\vec{k}_1)\\&\qquad\times\delta^{(3)}(\vec{k}\,'_C-\vec{k}_C)\langle\vec{q}_f|t(z)|\vec{q}_i\rangle\ ,\end{aligned} \tag{2.12}$$

where $t(z)$ is the pion-free nucleon scattering matrix. The meaning of various kinematic variables in the three sys-

TABLE I. Notation used for energies and momenta of the interacting particles.

	Arbitrary system	$A_{\text{c.m.}}$	$2_{\text{c.m.}}$
Initial (final) pion momentum	$\vec{p}$ ($\vec{p}\,'$)	$\vec{Q}$ ($\vec{Q}\,'$)	$\vec{q}_i$ ($\vec{q}_f$)
Initial (final) nuclear momentum	$\vec{\kappa}$ ($\vec{\kappa}\,'$)	$-\vec{Q}$ ($-\vec{Q}\,'$)	
Initial (final) target nucleon momentum	$\vec{k}_1$ ($\vec{k}\,'_1$)		$-\vec{q}_i$ ($-\vec{q}_f$)
Core momentum	$\vec{k}_C$ ($\vec{k}\,'_C$)		
Reaction energy (momentum)	E	E_{Ac} (p_{Ac})	z (p_{2c})

tems of our interest, namely in an arbitary system, in a pion-nucleus center-of-mass system ($A_{\text{c.m.}}$), and in the pion-nucleon center-of-mass system ($2_{\text{c.m.}}$), is apparent from Table I.

Now the potential matrix can be written as

$$\langle \vec{\kappa}',\vec{p}',n' \mid U(E) \mid n,\vec{p},\vec{\kappa}\rangle = (2\pi)^3\delta^{(3)}(\vec{p}'+\vec{\kappa}'-\vec{p}-\vec{\kappa})\langle \vec{Q}'n' \mid U_r(E_{Ac}) \mid n\vec{Q}\rangle \ , \tag{2.13}$$

where the potential matrix $U_r(E_{Ac})$ in $A_{\text{c.m.}}$ reads as

$$\langle \vec{Q}'n' \mid U_r(E_{Ac}) \mid n\vec{Q}\rangle = \frac{A-1}{(2\pi)^3}\int \exp\left[i\frac{A-1}{2A}(\vec{Q}'-\vec{Q})\cdot(\vec{r}'+\vec{r})+i\vec{v}\cdot(\vec{r}'-\vec{r})\right] \times Sp[\rho_{n'n}(\vec{r}',\vec{r})\langle \vec{q}_f \mid t(z) \mid \vec{q}_i\rangle]d^3v\, d^3r'd^3r \ . \tag{2.14}$$

Here, $\vec{r}'$ ($\vec{r}$) is the nucleon-core relative coordinate in the final (initial) state, $\rho_{n'n}(\vec{r}',\vec{r})$ is the nuclear density matrix, and the symbolic notation

$$Sp[\rho_{n'n}(\vec{r}',\vec{r})\langle \vec{q}_f \mid t(z) \mid \vec{q}_i\rangle] \equiv \sum_{\sigma_{1z},\sigma'_{1z},\tau_{1z},\tau'_{1z}} \rho_{n'n}(\vec{r}'\sigma'_{1z}\tau'_{1z},\vec{r}\sigma_{1z}\tau_{1z})\langle \vec{q}_f\sigma'_{1z}\tau_{1z} \mid t(z) \mid \vec{q}_i\sigma_{1z}\tau_{1z}\rangle$$

is adopted in Eq. (2.14) for the summation over the target nucleon spin and isospin projections. Momentum $\vec{v}$ denotes in Eq. (2.14) the mean relative nucleon-core momentum in the initial and final states and enters into the elementary pion-nucleon scattering matrix via

$$\vec{q}_f = \vec{Q}' - \frac{A-1}{2A}\frac{\mu}{\mathcal{M}}(\vec{Q}'+\vec{Q}) + \frac{\mu}{M}\vec{v} \equiv \vec{q}_{f0} + \frac{\mu}{M}\vec{v} \ , \tag{2.15}$$

$$\vec{q}_i = \vec{Q} - \frac{A-1}{2A}\frac{\mu}{\mathcal{M}}(\vec{Q}'+\vec{Q}) + \frac{\mu}{M}\vec{v} \equiv \vec{q}_{i0} + \frac{\mu}{M}\vec{v} \ ,$$

and

$$z = E_{Ac} - \frac{1}{2M}\frac{\mu}{\mathcal{M}}\frac{A}{A-1}\left[\vec{v} - \frac{A-1}{2A}(\vec{Q}'+\vec{Q})\right]^2 - U_C - \epsilon_B \ , \tag{2.16}$$

since the energy E is scaled as

$$E = E_{Ac} + \frac{(\vec{p}+\vec{\kappa})^2}{2(m+AM)} - \epsilon_B \ , \tag{2.17}$$

where $\epsilon_B > 0$ is the nucleon-core binding energy. Here, μ ($\mathcal{M}$) is the pion-nucleon (nucleus) reduced mass, and m and M are the pion and nucleon mass, respectively.

The potential matrix (2.14) exhibits the nonstatic and nonlocal features of pion-nucleus interaction. In the vicinity of the Δ_{33} resonance it describes the free Δ_{33} isobar propagation between points $\vec{r}'$ and $\vec{r}$ much like the isobar-doorway model.[11] However, there is no dynamical distortion[13] of the isobar propagation in Eq. (2.14), which has been taken into account at least phenomenologically (via the spreading potential) in the recent isobar-doorway calculations of pion elastic and inelastic scattering by Lenz.[14] In our model, a portion of the Δ-core dynamics is taken into account explicitly via solving the coupled channel system (2.7) within the P space.

In practical calculations, we have used approximations that lead to a more static picture of the π-N subsystem propagation. First, we set

$$-\frac{1}{2M}\frac{\mu}{\mathcal{M}}\frac{A}{A-1}v^2 - U_C - \epsilon_B = 0 \tag{2.18}$$

in Eq. (2.16). This represents a reasonable approximation for energies E_{Ac} considerably higher than the mean kinetic energy of the nucleon-core relative motion. Second, we neglected the terms containing $\vec{v}$ in Eqs. (2.15) and (2.16). In other words, we replace the actual momentum of a target nucleon in the initial and final states by the effective values

$$\vec{k} = \frac{\vec{\kappa}}{A} + \frac{A-1}{2A}(\vec{Q}'-\vec{Q}) \ , \quad \vec{k}' = \frac{\vec{\kappa}'}{A} - \frac{A-1}{2A}(\vec{Q}'-\vec{Q}) \ , \tag{2.19}$$

respectively. Such an approximation is very good for diagonal ($n=n'$) matrix elements[11] of $U_r(E_{Ac})$, and its validity for nondiagonal elements was investigated in detail by Lenz *et al.*[2] In some instances the last approximation can yield for $n \neq n'$ substantially different forward ($\vec{Q}=\vec{Q}'$) and/or backward ($\vec{Q}=-\vec{Q}'$) matrix elements of the "exact" (2.14) and approximate potential matrix

$$\langle \vec{Q}'n' \mid U_r(E_{Ac}) \mid n\vec{Q}\rangle = (A-1)Sp[F_{n'n}(\vec{Q}'-\vec{Q})\langle \vec{q}_{f0} \mid t(z_0) \mid \vec{q}_{i0}\rangle] \ , \tag{2.20}$$

since the latter may vanish there due to symmetry of the nuclear form factors

$$F_{n'n}(\vec{Q}'-\vec{Q}) = \int e^{i(A-1/A)(\vec{Q}'-\vec{Q})\cdot\vec{r}}\rho_{n'n}(\vec{r},\vec{r})d^3r \ . \tag{2.21}$$

Therefore, our approximate potential matrix is expressed in the "factorized" form (2.20) as a combination of nuclear form factors and the elementary πN amplitude evaluated at effective pion momenta $\vec{q}_{f0}$ and $\vec{q}_{i0}$ [see Eq. (2.15)], and the effective pion energy

$$z_0 = E_{Ac} - \frac{1}{8M}\frac{\mu}{\mathcal{M}}\frac{A-1}{A}(\vec{Q}'+\vec{Q})^2 \tag{2.22}$$

and the only $m/M \sim \frac{1}{7}$ terms retained in our calculations are those associated with the "angle transformation."[15] It can be shown[11] that Eqs. (2.20) and (2.22) describe the propagation of the πN subsystem between points $\vec{r}'$ and $\vec{r}$; however, the density matrix $\rho_{n'n}(\vec{r}',\vec{r})$ is approximated

by its diagonal element $\rho_{n'n}(\frac{1}{2}(\vec{r}'+\vec{r}),\frac{1}{2}(\vec{r}'+\vec{r})) \equiv \rho_{n'n}(\frac{1}{2}(\vec{r}'+\vec{r}))$.

The nuclear structure input in Eq. (2.20) can be extracted to a large extent from the electron scattering experiments, whereas a reliable evaluation of the "exact" expression (2.14) requires rather detailed knowledge of the nuclear wave functions of the ground and corresponding excited states, which is rarely available.

C. Pion-nucleon amplitude

The pion-nucleon scattering matrix can be expressed as

$$\langle \vec{q}_{f0} \mid t(z_0) \mid \vec{q}_{i0} \rangle = -\frac{2\pi}{\mu}\{A_{00}+(\vec{t}\cdot\vec{\tau})A_{01}+i\vec{\sigma}\cdot[\vec{v}_f\times\vec{v}_i](A_{10}+(\vec{t}\cdot\vec{\tau})A_{11})\} , \tag{2.23}$$

where, e.g., $\vec{v}_f=\vec{q}_{f0}/\mid\vec{q}_{f0}\mid$, $\vec{t}$ is the pion isospin operator, and $\vec{\sigma}$ and $\vec{\tau}$ are the spin and isospin operators of the target nucleon, respectively. Furthermore, $A_{ST} \equiv A_{ST}(\cos\Theta)$ $(S=0,1;\ T=0,1)$ are usual[16] combinations of the pion-nucleon off-energy-shell partial amplitudes $f_{l\alpha}^{(\pm)}$ and $\cos\Theta=\vec{v}_f\cdot\vec{v}_i$. Here, l is the pion-nucleon angular momentum, $\alpha=\frac{1}{2}$ or $\frac{3}{2}$ is the isospin of the πN system, and $(\pm)$ corresponds to the total spin $j=l\pm\frac{1}{2}$ of the system.

We used the separable form

$$f_{l\alpha}^{(\pm)}=f_{l\alpha}^{(\pm)}(q_{f0},q_{i0},z_0)=\frac{v_{l\alpha}^{(\pm)}(q_{f0})v_{l\alpha}^{(\pm)}(q_{i0})}{[v_{l\alpha}^{(\pm)}(p_{2c})]^2} \times f_{l\alpha}^{(\pm)}(p_{2c},p_{2c},z_0) \tag{2.24}$$

of the partial amplitudes. The on-shell values $f_{l\alpha}^{(\pm)}(p_{2c},p_{2c},z_0)$, $p_{2c}=\sqrt{2\mu z_0}$ were calculated according to Ref. 17. The nonlocality of the πN amplitude is characterized by the function $v_{l\alpha}^{(\pm)}(p)$, $p=q_{f0},q_{i0}$, and p_{2c}. The parametrization

$$v_{l\alpha}^{(\pm)}(p)=\frac{p^l}{[1+(r_0p)^2]^2} \tag{2.25}$$

was utilized in our calculations. The value $r_0=0.47$ fm leads to $v_{1(3/2)}^{(\pm)}(p)$, which is very much like the πN separable potential[18] in the corresponding (resonating) particle wave.

With the help of parametrization (2.23), the resulting expression for the potential matrix reads as

$$\langle \vec{Q}'n' \mid U_r(E_{Ac}) \mid n\vec{Q}\rangle = -\frac{2\pi}{\mu}(A-1)\sum_{\substack{S,T=0,1\\ \gamma\delta}} A_{ST} i^{(S)}[\vec{v}_f\times\vec{v}_i]_\gamma^{(S)} t_\delta^{(T)} Sp[\tau_\delta^{(T)}\sigma_\gamma^{(S)}F_{n'n}(\vec{Q}'-\vec{Q})] . \tag{2.26}$$

We defined $\sigma_\gamma^{(0)}=1$ for $S=0$ and $\sigma_\gamma^{(1)}=\sigma_\gamma$ for $S=1$. Similar relations hold also for $i^{(S)}$, $\tau_\delta^{(T)}$, $t_\delta^{(T)}$, $\sigma_\gamma^{(S)}$, and $[\vec{v}_f\times\vec{v}_i]_\gamma^{(S)}$.

D. Relativistic corrections

Since our calculations will be performed in the energy interval $100\lesssim E_{Ac}\lesssim 250$ MeV, it is necessary to evaluate relativistic kinematical corrections. Doing so we follow the prescriptions of Ref. 19.

(i) The nonrelativistic Green's function

$$\langle \vec{Q} \mid G_{nn}(E) \mid \vec{Q}\rangle = 2\mathscr{M}(p_{Ac}^2-Q^2-2\mathscr{M}e_n+i\epsilon)^{-1}$$

is replaced in Eq. (2.7) by

$$\langle \vec{Q} \mid G_{nn}(E) \mid \vec{Q}\rangle = [\mathscr{E}-\mathscr{E}_n(Q)+i\epsilon]^{-1} , \tag{2.27}$$

where e_n is the nuclear excitation energy ($e_0=0$) and

$$\mathscr{E}=\mathscr{E}_0(Q_0)=E_\pi(Q_0)+E_A^{(0)}(Q_0)$$

is the total reaction energy ($\mid\vec{Q}_0\mid\equiv p_{Ac}$), and

$$E_\pi(Q)=(Q^2+m^2)^{1/2}$$

and

$$E_A^{(n)}(Q)=[Q^2+(M_A+e_n)^2]^{1/2} .$$

Furthermore, $\mathscr{E}_n(Q)=E_\pi(Q)+E_A^{(n)}(Q)$ holds and the relation $\mathscr{E}-\mathscr{E}_n(Q_n)=0$ defines the pion on-shell (asymptotic) momentum in an nth channel.

It can easily be shown that

$$\mathscr{E}-\mathscr{E}_n(Q)\equiv\mathscr{E}_n(Q_n)-\mathscr{E}_n(Q)=\frac{Q_n^2-Q^2}{2\mathscr{M}(n,Q)} , \tag{2.28}$$

where

$$\frac{1}{\mathscr{M}(n,Q)}=2\frac{\mathscr{E}^2+\mathscr{E}_n^2(Q)}{[\mathscr{E}+\mathscr{E}_n(Q)][E_\pi(Q_n)E_A^{(n)}(Q_n)+E_\pi(Q)E_A^{(n)}(Q)]} . \tag{2.29}$$

Therefore, the relativistically modified system (2.7) again has the form of the coupled Lippmann-Schwinger equations

$$\langle \vec{Q}'n' \mid F(\mathscr{E}) \mid 0\vec{Q}_0\rangle = \langle \vec{Q}'n' \mid V(z_0) \mid 0\vec{Q}_0\rangle - \frac{1}{2\pi^2}\sum_{n\in P}\int \frac{\langle \vec{Q}'n' \mid V(z_0) \mid n\vec{Q}''\rangle\langle \vec{Q}''n \mid F(\mathscr{E}) \mid 0\vec{Q}_0\rangle}{Q_n^2-Q''^2+i\epsilon}d^3Q'' , \tag{2.30}$$

where, however,

$$\langle \vec{Q}'n' \mid F(\mathscr{E}) \mid 0\vec{Q}_0\rangle = -\frac{1}{2\pi}[\mathscr{M}(n',Q')\mathscr{M}(0,Q_0)]^{1/2}\langle \vec{Q}'n' \mid T(\mathscr{E}) \mid 0\vec{Q}_0\rangle \ , \tag{2.31}$$

and [see Eq. (2.26)]

$$\langle \vec{Q}'n' \mid V(z_0) \mid n\vec{Q}\rangle = W_{n'n}(Q',Q)\sum_{ST\gamma\delta} A_{ST}i^{(S)}[\vec{v}_f\times v_i]^{(S)}_{\gamma}t^{(T)}_{\delta}Sp[\sigma^{(S)}_{\gamma}\tau^{(T)}_{\delta}F_{n'n}(\vec{Q}'-\vec{Q})] \ . \tag{2.32}$$

The transformation factor

$$W_{n'n}(Q',Q)=\left[\frac{\mathscr{M}(n',Q')\mathscr{M}(n,Q)}{\mu(Q',k')\mu(Q,k)}\right]^{1/2} \tag{2.33}$$

was obtained using Eq. (2.29) and the relativistic relation between the elementary πN-scattering amplitude and the πN amplitude in $2_{\text{c.m.}}$. We denoted

$$\mu(Q',k')=E_{\pi}(Q')E_N(k')\{[E_{\pi}(Q')+E_N(k')]^2 - (\vec{Q}'+\vec{k}')^2\}^{1/2} \ , \tag{2.34}$$

where the nucleon momentum $\vec{k}'$ is given by Eq. (2.19). An analogous relation holds also for $\mu(Q,k)$.

(ii) The $2_{\text{c.m.}}$ momenta $\vec{q}_{f0}$ and $\vec{q}_{i0}$ are given by the approximative relativistic formulas

$$\vec{q}_{f0}=\mu(Q',k')\left[\frac{\vec{Q}'}{E_{\pi}(Q')}-\frac{\vec{k}'}{E_N(k')}\right], \qquad \vec{q}_{i0}=\mu(Q,k)\left[\frac{\vec{Q}}{E_{\pi}(Q)}-\frac{\vec{k}}{E_n(k)}\right], \tag{2.35}$$

the validity of which was discussed in Refs. 19 and 20.

(iii) The relativistic generalization of the effective energy z_0 was postulated in the spirit of the "three-body" model. For instance, for the matrix element (2.32), it has the form

$$z_0=\mathscr{E}+m+M-\left\{(m+M)^2+\left[\frac{A-1}{2A}(\vec{Q}'+\vec{Q})\right]^2\right\}^{1/2} - \left\{(A-1)^2M^2+\left[\frac{A-1}{2A}(\vec{Q}'+\vec{Q})\right]^2\right\}^{1/2} , \tag{2.36}$$

which in the nonrelativistic limit coincides with (2.22).

E. Method of calculation

As a next step in solving system (2.30) we perform the usual decomposition in pion-nucleus partial waves. If, furthermore, the Green's function is split,

$$\frac{1}{Q_n^2-Q^2+i\epsilon}=\frac{P}{Q_n^2-Q^2}-i\pi Q_n\delta(Q_n-Q) \ , \tag{2.37}$$

into the δ function (pion on-shell propagation) and principal value part, we have

$$F^{jIP}_{nL',0L}(Q',Q_0)=\omega^{jIP}_{nL',0L}(Q',Q_0)+i\sum_{m,L''}{}' Q_m\omega^{jIP}_{nL',mL''}(Q',Q_m)F^{jIP}_{mL'',0L}(Q_m,Q_0) - \frac{2}{\pi}\sum_{m,L''}\int_0^{\infty}\frac{Q''^2\omega^{jIP}_{nL',mL''}(Q',Q'')F^{jIP}_{mL'',0L}(Q'',Q_0)-Q_m^2\omega^{jIP}_{nL',mL''}(Q',Q_m)F^{jIP}_{mL'',0L}(Q_m,Q_0)}{Q_m^2-Q''^2}dQ'' \ . \tag{2.38}$$

Summation in the δ-function term runs over the open channels only; this is denoted by a prime. We used the same regularization of the principal value integral as suggested by Haftel and Tabakin[21] in the elastic scattering case. The partial waves are labeled by the total pion-nucleus spin j (e.g., $\vec{j}=\vec{L}'+\vec{J}_n=\vec{L}''+\vec{J}_m$), isospin I (e.g., $\vec{I}=\vec{1}+\vec{T}_n=\vec{1}+\vec{T}_m$), and parity P. Finally, L, L', and L'' are pion-nucleus angular momenta in corresponding channels. The dependence of the potential matrix on energy z_0 is not shown explicitly in (2.38).

Starting from Eq. (2.32), we obtain the elements of the potential matrix in the form

$$\omega^{jIP}_{n'L',nL}(Q',Q)=W_{n'n}(Q',Q)(A-1)\sum_{\substack{lrpN\\CDST}}(-1)^{1+T'_n+I+J'_n+j+p+r+N}([LL'N])^{1/2}[lrCD] \times\left[2\cdot3^T\cdot6^S\cdot\begin{bmatrix}2l\\2p\end{bmatrix}\right]^{1/2}i^{L'-L+l}Q'^pQ^{l-p}\begin{Bmatrix}1 & 1 & T\\ T'_n & T_n & I\end{Bmatrix}\begin{Bmatrix}L & L' & N\\ J_n & J'_n & j\end{Bmatrix}\begin{Bmatrix}L & L' & N\\ S & S & S\\ C & D & l\end{Bmatrix} \times\begin{Bmatrix}D & C & l\\ l-p & p & r\end{Bmatrix}\begin{bmatrix}L & S & C\\ 0 & 0 & 0\end{bmatrix}\begin{bmatrix}p & D & r\\ 0 & 0 & 0\end{bmatrix}\begin{bmatrix}l-p & C & r\\ 0 & 0 & 0\end{bmatrix} \times\tfrac{1}{2}\int_{-1}^{1}P_r(\cos\vartheta)A_{ST}(\cos\vartheta)H^{ST}_{IN}(\cos\vartheta,n',n)d(\cos\vartheta) \ . \tag{2.39}$$

Here $P_r(\cos\vartheta)$ are Legendre polynomials. $A_{ST}(\cos\vartheta)$ are combinations of πN amplitudes, and the nuclear structure enters into (2.39) via scalar quantities,

$$H_{lN}^{ST}(\cos\vartheta,n',n)=\sqrt{4\pi}\sum_{\substack{T_{nz}T'_{nz}\gamma\delta\\ J_{nz}J'_{nz}\nu}}\sqrt{[N]}(-1)^{J'_n-J'_{nz}+T'_n-T'_{nz}-l+S-\nu}$$

$$\times\begin{bmatrix} T'_n & T & T_n\\ -T'_{nz} & \delta & T_{nz}\end{bmatrix}\begin{bmatrix} J'_n & N & J_n\\ -J'_{nz} & \nu & J_{nz}\end{bmatrix}\begin{bmatrix} l & S & N\\ \lambda & \gamma & -\nu\end{bmatrix}$$

$$\times\int q^{-l}j_l\left[\frac{A-1}{A}qr\right]Y^*_{l\lambda}(\hat{r})Sp[\tau_\delta^{(T)}\sigma_\gamma^{(S)}\rho_{n'n}(\vec{r})]d^3r\ , \tag{2.40}$$

where $\vec{q}=\vec{Q}'-\vec{Q}$ and $\cos\vartheta=\vec{Q}'\cdot\vec{Q}/(Q'Q)$.

The system (2.38) was solved using the matrix inversion method.[21] The Coulomb interaction (finite size nuclear charge) was taken into account only in the elastic scattering matrix elements ($n'=n=0$). The elastic scattering phase shifts were obtained by using the matching procedure of Vincent and Phatak.[22]

III. NUCLEAR TRANSITION DENSITIES

The transition densities $\rho_{n'n}(\vec{r})$ in (2.40) should normally be calculated within some nuclear model wave functions of the states $|n\rangle$ and $|n'\rangle$. Unfortunately, the models currently used are typically unable to reproduce, e.g., the observed electron scattering data. Since the difference between theoretical and experimental (e,e') results are sometimes really large, it would be meaningless to use such inaccurate nuclear structure information as input for the (π,π') calculations. Instead we wish to extract $\rho_{n'n}$ from the known cross sections of inelastic scattering of electrons on a given nucleus. From electron-scattering experiments we can obtain only transition densities $\rho_{n'0}(\vec{r})$. When the calculations with pions in the framework of the coupled-channel (CC) method are performed, one needs the densities $\rho_{n'n}(\vec{r})$ with, generally, $n\neq0$. To determine them, it is necessary to start with some nuclear model.

One can see that expression (2.40) contains the reduced matrix elements of the tensor operator

$$M^{(T)}_{N\nu,\delta}=q^{-l}j_l(qr)[Y_l\otimes\sigma^{(S)}]_{N\nu}\tau^{(T)}_\delta$$

between the nuclear states characterized by indices n' and n. In ^{24}Mg, ^{26}Mg, and ^{28}Si approximately half of the $2s1d$ shell is occupied by nucleons; the nuclei are therefore believed to be deformed, and we use the collective axial-symmetric rotor model[23] for their description. In the framework of this model the nuclear state is characterized by ket $|n\rangle=|J_nK_nJ_{nz}\rangle$, where K_n is the projection of J_n on the symmetry axis of a nucleus (we omit the isospin part). The reduced matrix element of the tensor operator $M_N^{(T)}$ between these states can be written as[23]

$$\langle J_{n'}K_{n'}||M_N^{(T)}||J_nK_n\rangle=\sqrt{[J_n]}\left[\begin{bmatrix} J_{n'} & N & J_n\\ -K_{n'} & K_{n'}-K_n & K_n\end{bmatrix}(-)^{J_{n'}-K_{n'}}\langle K_{n'}|M^{(T)}_{NK_{n'}-K_n}|K_n\rangle\right.$$

$$\left.+(-)^{J_n+K_n}\begin{bmatrix} J_{n'} & N & J_n\\ -K_{n'} & K_{n'}+K_n & -K_n\end{bmatrix}(-)^{J_{n'}-K_{n'}}\langle K_{n'}|M^{(T)}_{NK_{n'}+K_n}|K_n\rangle\right] \tag{2.41a}$$

for $K_n\neq0$, $K_{n'}\neq0$ and

$$\langle J_{n'}K_{n'}||M_N^{(T)}||J_nK_n\rangle=\sqrt{[J_n]}\begin{bmatrix} J_{n'} & N & J_n\\ -K_{n'} & K_{n'} & 0\end{bmatrix}(-)^{J_{n'}-K_{n'}}\langle K_{n'}|M^{(T)}_{NK_{n'}}|0\rangle\begin{cases}\sqrt{2}\text{ for }K_{n'}\neq0\\ 1\text{ for }K_{n'}=0\ .\end{cases} \tag{2.41b}$$

It is to be noted that the radial part of the reduced matrix element which contains the Bessel function $j_l(qr)$ rapidly tends to zero (for not too large q) with an increasing value of l. Therefore we restricted our numerical calculations to $l\leq4$ and $N\leq4$. Indeed we also assume that the contribution of spin-dependent operators $[Y_l\otimes\sigma]_N$ can be neglected. These facts allow us to rewrite for $K\leq2$ expressions (2.41a) and (2.41b) in the more compact form

$$\langle J_{n'}K_{n'}||M_N^{(T)}||J_nK_n\rangle=[(2-\delta_{K_nK_{n'}})(2J_n+1)]^{1/2}(-1)^{J_{n'}-K_{n'}}\begin{bmatrix} J_{n'} & N & J_n\\ -K_{n'} & K_{n'-K_n} & K_n\end{bmatrix}\langle K_{n'}|M^{(T)}_{NK_{n'}-K_n}|K_n\rangle\ . \tag{2.42}$$

In terms of (2.42) one can determine the intrinsic matrix elements $\langle K_{n'} | M^{(T)}_{NK_{n'}-K_n} | K_n \rangle$ from experimentally known (e,e') form factors and eventually obtain all form factors needed for CC calculations of the (π,π') reactions. Doing so we always assumed that the proton and neutron densities are the same. Therefore, we arrived at the relation

$$\langle K_{n'} | M^{(1)}_{NK_{n'}-K_n} | K_n \rangle = \frac{2}{A}\sqrt{T(T+1)}\langle K_{n'} | M^{(0)}_{NK_{n'}-K_n} | K_n \rangle \quad (2.43)$$

between the isoscalar and isovector reduced matrix elements. Equation (2.43) holds in the case $T_{n'}=T_n=T$; only such transitions are assumed in our examples.

In ^{24}Mg four positive-parity isoscalar ($T=0$) states are excited in (π,π'): $J=K=0$ (g.s.); $J=2$, $K=0$ (1.37 MeV); $J=2$, $K=2$ (4.24 MeV); $J=4$, $K=2$ (6.01 MeV). The CC calculation involving all these levels needs 29 nuclear form factors which can be determined from five electron form factors by the method proposed above. In the case of ^{26}Mg we considered two positive-parity $T=1$ states in the CC calculation: $J=K=0$ (g.s.) and $J=2$, $K=0$ (1.81 MeV) that necessitates five form factors to be determined from the two electron ones. Three $T=0$ states, $J=K=0$ (g.s); $J=2$, $K=0$ (1.78 MeV); and $J=4$, $K=0$ (4.62 MeV) have been included into the CC calculation with ^{28}Si. Eleven form factors needed have been obtained by the aforementioned procedure from three electron ones.

For each transition we have fitted the constants of the two-parameter Fermi density ρ_{2pF} (or $r^{L-1}d\rho_{2pF}/dr$ for inelastic scattering) so that the corresponding Fourier transforms describe the experimental electron form factors for all nuclei considered (^{24,26}Mg, ^{28}Si, and also ^{18}O).

IV. RESULTS AND DISCUSSION

In this section we present the results calculated for pion elastic and inelastic scattering by ^{24,26}Mg and ^{28}Si within the coupled-channel formalism. These results are compared with the existing experimental data and with our DWIA calculations.

The aim of the comparison is to reveal the importance of multistep mechanisms in pion-nucleus scattering in the region of light deformed nuclei. In some instances the results of coupled-channel calculations are also displayed in which the pion propagation off the pion-nucleus energy shell is disregarded. The procedure consists in neglecting the principal-value part in the decomposition (2.37) of the Green's function. In such a case, the pion-nucleus scattering amplitudes are solutions of the system of algebraic equations

$$F^{jIP}_{nL',0L}(Q',Q_0)=\omega^{jIP}_{nL',0L}(Q',Q_0) + i\sum_{mL''}{}'Q_m\omega^{jIP}_{nL',mL''}(Q',Q_m) \times F^{jIP}_{mL'',0L}(Q_m,Q_0)$$

that replaces the system of integral equations (2.38).

It has already been shown[24] that the on-shell approximation reproduces all basic features of the pion-nucleus scattering in the Δ_{33}-resonance region surprisingly well. The comparison of the full coupled-channel calculations with those containing only the pion on-shell propagation indicates the role of the pion off-shell scattering mechanisms which are rather strongly model dependent.

The nuclear densities used as input in our CC calculations are determined from the electron scattering experiments. We have assumed that the proton and neutron densities are the same for all the nuclei considered. No attempt was made to modify the nuclear densities for better fitting to the pion-nucleus scattering data.

A. π^+-^{24}Mg scattering

In Fig. 1 the calculated results are compared with the experimental data for π^+ elastic and inelastic scattering on ^{24}Mg at $E_\pi=180$ MeV. The ground state as well as all the excited states considered are the isoscalar ($T=0$) levels. The results of our complete CC calculations are denoted by full lines. The dashed lines were obtained

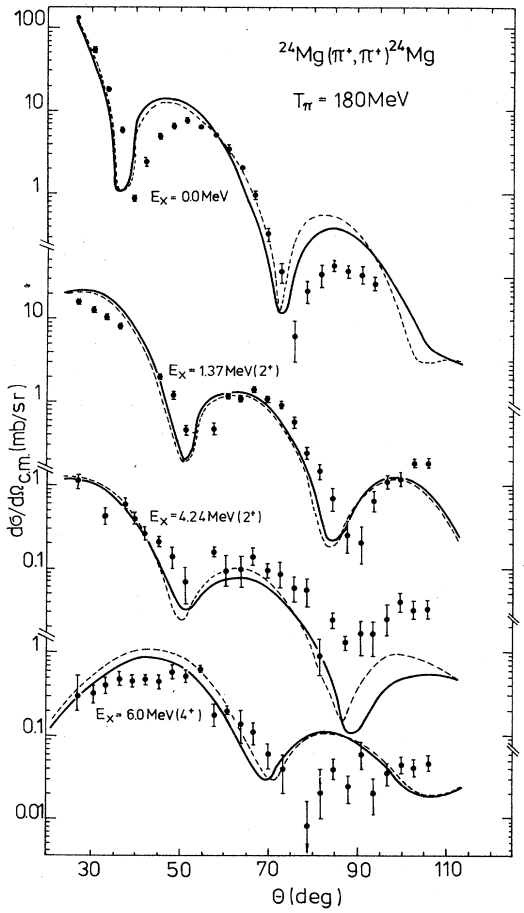

FIG. 1. Comparison of calculated results with experimental data (Ref. 26) for π^+ elastic and inelastic scattering on ^{24}Mg. —— four coupled channels; — — — channel coupling "turned off."

when the channel coupling was turned off. Therefore, the dashed lines represent the optical model and DWIA results for pion elastic and inelastic scattering, respectively. It may be concluded that qualitatively the calculated results reproduce the experimental data well in the region of small scattering angles. There are definite discrepancies in the region of the first minimum, and the diffractive patterns of the calculated curves are somewhat shifted to smaller scattering angles as compared with experiment. The difference between the full and dashed curves is very small; therefore the multistep processes play only a minor role in both the pion elastic scattering and those inelastic reactions that were considered in our calculations.

It should be noticed that there are small differences between our present and previous CC calculations. In extracting the nuclear densities from electron scattering data in our preceding paper[25] we erroneously omitted the proton form factor.

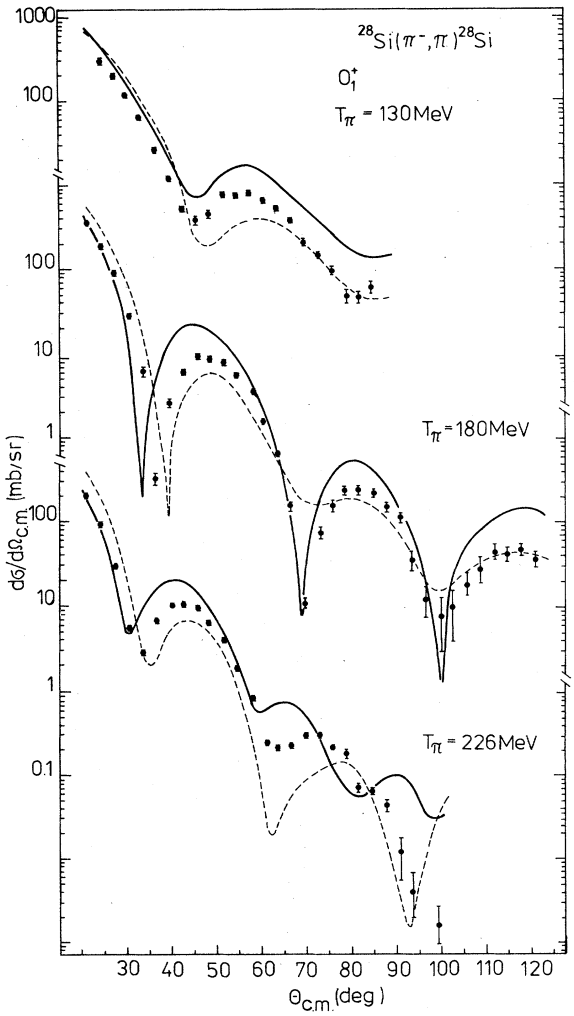

FIG. 2. Comparison of coupled-channel results with experimental data (Ref. 27) for π^- elastic scattering on ^{28}Si. —— three coupled channels, complete Green's function; — — — three coupled channels, pion on-shell only propagation.

There are also some differences between our DWIA results and those of Wiedner *et al.*,[26] especially as far as the heights of secondary peaks are concerned. This is not surprising, since these authors used a crude model of the nuclear structure, where a certain "deformation parameter" β_L should be fitted. Nevertheless, the diffractive structure obtained in Ref. 26 is also shifted towards small scattering angles as compared with experiment, in much the same way as our results.

B. $\pi^{\pm}$-^{28}Si scattering

In Fig. 2 the coupled-channel results (full lines) obtained for the π^--^{28}Si elastic scattering are compared with the experimental data at three energies. Assuming only the pion on-shell propagation we arrived at the results shown in Fig. 2 by dashed lines. The one-channel (optical-model) calculations are not shown in Fig. 2, since they differ only slightly from the full lines. An analogous comparison of the calculated and experimental results is performed in Figs. 3 and 4 for pion inelastic scattering to the $(2_1^+,0)$ and $(4_1^+,0)$ levels, respectively.

As in Fig. 1, we can observe that CC calculations produce a diffractive structure, for π-^{28}Si elastic and inelastic scattering, which is shifted somewhat towards low scattering angles as compared with experiment. Such a shift might be removed[26] by slightly changing the diffusivity parameter of the nuclear densities. However, as follows from the comparison of our full CC and pion on-shell re-

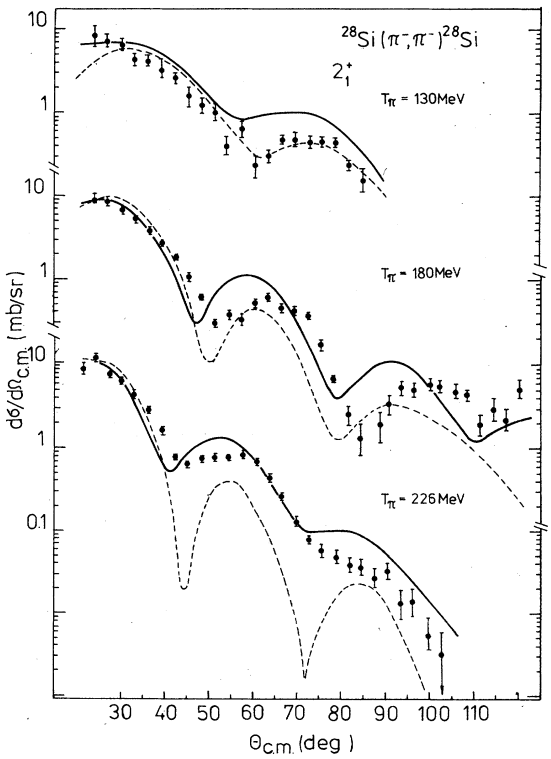

FIG. 3. Comparison of coupled-channel results with experimental data (Ref. 27) for π^--^{28}Si inelastic scattering to the $(2_1^+,0)$ level. The meaning of the curves is the same as in Fig. 2.

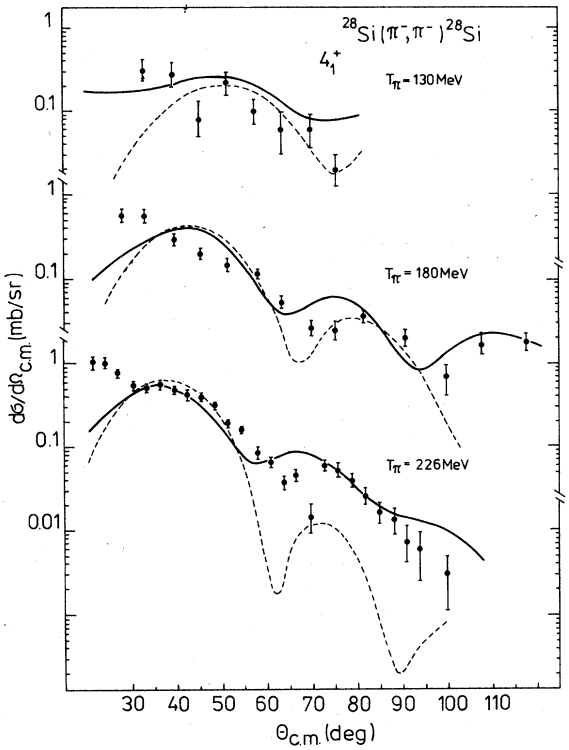

FIG. 4. Comparison of coupled-channel results with experimental data (Ref. 27) for π^--^{28}Si inelastic scattering to the $(4_1^+,0)$ level. The meaning of the curves is the same as in Fig. 2.

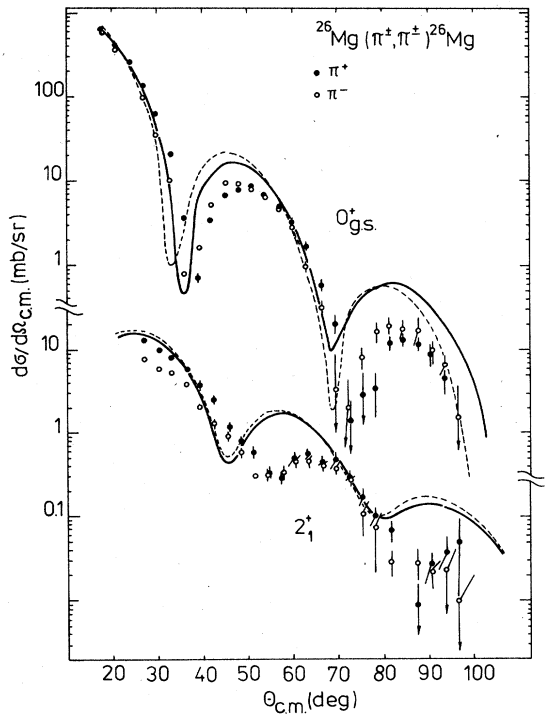

FIG. 5. Comparison of coupled-channel results with experimental data (Ref. 28) for $\pi^\pm$-^{26}Mg elastic and inelastic scattering. —— π^+ scattering; — — — π^- scattering.

sults, the position of diffractive minima is also affected by the off-shell effects.

One can conclude that the CC calculations reproduce rather well the experimental data in the region of small scattering angles. The only exception is the inelastic scattering to the $(4_1^+,0)$ level, Fig. 4, where there are some discrepancies for angles $\vartheta \lesssim 30°$. As a rule, the CC calculations give a better overall description of the experimental data than the on-shell calculations. This is apparent especially for the highest energy $E_\pi = 226$ MeV data shown in Figs. 2—4. Nevertheless, the positions of diffractive minima are sometimes better reproduced by the less model-dependent on-shell calculations.

C. $\pi^\pm$-^{26}Mg scattering

In Fig.5 the CC results obtained for the ground state elastic π^+-^{26}Mg scattering and for the π^+-^{26}Mg inelastic scattering to the excited $(2_1^+,1)$ state are shown by the full lines. Analogous results obtained for the π^--^{26}Mg scattering are given by dashed lines, and the comparison with the experimental data at $E_\pi = 180$ MeV is performed.

In contrast with the two previously discussed nuclei, ^{24}Mg and ^{28}Si, we have to deal with two isovector levels in the case of ^{26}Mg. Therefore, the potential matrix (2.26) contains now, aside from the usual isoscalar term, also the isovector part that is associated with the isovector part A_{01} of the πN amplitude. Thus the difference between our π^+- and π^--^{26}Mg results is caused by Coulomb and strong interaction effects.

Though the forward elastic scattering is fairly well reproduced by our calculaitons, the calculated diffractive structure is shifted towards low scattering angles as compared with experiment. The shift is smaller than 5° in the case of elastic scattering and it amounts to about 15° for the inelastic scattering. In our calculations the first diffractive minimum in the elastic π^--^{26}Mg scattering occurs at a somewhat smaller angle than in the elastic π^+-^{26}Mg one. The same trend is also observed in the experiment; however, the quantitative description of the effect is rather poor. The calculations do not reproduce a rather large difference between the π^+- and π^--inelastic data in the first-peak region. Such a difference seems to indicate that the proton and neutron densities differ for the $(2_1^+,1)$ state.

The difference between CC calculations and optical-model or DWIA ones is again very small, and it is not shown in Fig. 5.

As for the comparison of our calculations and the experimental data, a word of caution is in order. The electromagnetic form factors from which we extract our nuclear structure input are experimentally known in different (and unfortunately rather narrow) intervals of transferred momentum for different nuclei and nuclear transitions. The best experimental data are available for ^{24}Mg. Both the electron elastic[30] and inelastic[31] form factors are measured up to $q \sim 2.1$ fm^{-1}. Such a transferred momentum occurs in pion-nucleus scattering of $E_\pi = 180$

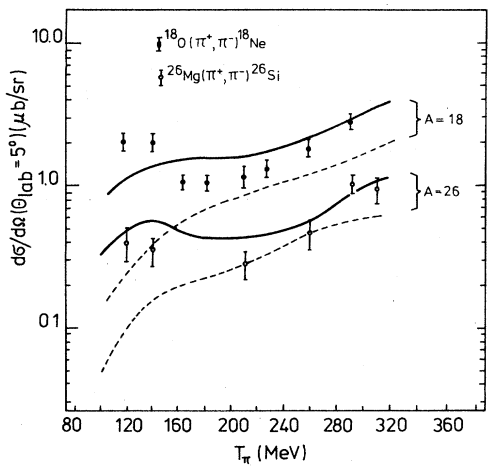

FIG. 6. Double-analog transitions $^{18}O(\pi^+,\pi^-)^{18}Ne$ and $^{26}Mg(\pi^+,\pi^-)^{26}Si$. Comparison of the calculated results with experimental data (Ref. 29) for differential cross sections at $\vartheta_\pi^{lab}=5°$. —— complete Green's function; — — — pion on-shell only propagation.

MeV for the scattering angle $\vartheta \lesssim 65°$. Electron data[30,32] of almost comparable quality are available for the ^{28}Si nucleus. The least favorable situation occurs for ^{26}Mg, where the elastic[30] and inelastic[33] form factors are known only up to $q \sim 1.15$ fm^{-1}. This corresponds to the pion scattering angle $\vartheta \lesssim 28°$ for $E_\pi = 180$ MeV. In view of this, it is not surprising that our calculations agree better with pion scattering data on ^{24}Mg than in the case of the ^{26}Mg nucleus.

D. Double-charge-exchange reaction $^{26}Mg(\pi^+,\pi^0)^{26}Si$

We applied our model also to the double-analog transition $^{26}Mg(\pi^+,\pi^-)^{26}Si$ which has been recently measured at $\vartheta = 5°$ for several energies around the Δ_{33} resonance. The comparison of the CC result and experimental data[29] is done in Fig. 6. The agreement between the calculated and experimental results is very good. Also, in this case the channel coupling plays a minor role. The one-channel (ground state) calculations, not shown in Fig. 6, differ from the full line typically by 5 percent. Our model certainly provides a better description of the experimental data than the Glauber model calculations[6] (irrespective of whether the meson exchange current corrections are taken into account or not). The pion on-shell calculations (dashed line) are in rather strong disagreement with the experiment, especially below and above the resonance. Such a situation is typical for a pion double-analog transition. This is demonstrated by our one-channel calculations of the $^{18}O(\pi^+,\pi^-)^{18}Ne$ reaction.

The agreement between the calculated and experimental results for the $^{26}Mg(\pi^+,\pi^-)^{26}Si$ reaction indicates that the assumption $\rho_p(r) \approx \rho_n(r)$ is fulfilled for the ^{26}Mg ground state within a reasonable accuracy. It is encouraging that the model accounts for both the forward elastic and forward $^{26}Mg(\pi^+,\pi^-)^{26}Si$ data which differ by six orders of magnitude, without any adjustment of parameters.

On the other hand, we are not able to correctly reproduce the dip position in the differential cross section of the $^{18}O(\pi^+,\pi^-)^{18}Ne$ and $^{26}Mg(\pi^+,\pi^-)^{26}Si$ reactions, which takes place at $\Theta \sim 20°$. Similar to other calculations that use only the analog intermediate states[36] or several nonanalog ones,[37] our calculated minimum is shifted considerably towards the large scattering angles. To account for the differential cross sections of DCE reactions, one should provide room in the model for substantial core excitations during the reaction, as the results of Ref. 8 seem to indicate.

V. CONCLUSION

We have demonstrated that the multiple-scattering formalism is capable of explaining the pion-scattering data on representative *s-d* shell nuclei in the vicinity of the Δ_{33}-resonance energy. The *conditio sine qua non* for that is the realistic nuclear structure input. In many transitions the calculated cross sections tend to differ considerably with data in the q range (e.g., for $q \geq 1$ fm^{-1} corresponding to $\Theta \gtrsim 30°$ at $E_\pi = 160$ MeV) where the nuclear density is not fixed by the measured (e,e') form factors. It seems that at present the most important theoretical task should be a development of the new models of the wave functions for the nuclear initial and final states capable of providing the necessary detailed information.

The calculation provides a justification of the DWIA method for the nuclear transitions considered and at energies near the Δ_{33} resonance. Our earlier experience with the *p*-shell nuclei supports, however, the possible importance of the strong channel coupling at lower ($E_\pi \lesssim 100$ MeV) energies. Data for the (π,π') reaction on Mg and Si isotopes at such energies would be welcome.

Technically, a very simple on-shell variant of our formalism which actually solves a system of algebraic rather than integral equations seems to be very well suited for quick estimates in the Δ_{33}-resonance region of energies.

The forward double-charge exchange data for the double-analog transitions $^{18}O(\pi^+,\pi^-)^{18}Ne$ and $^{26}Mg(\pi^+,\pi^-)^{26}Si$ have been reproduced unexpectedly well despite the extreme crudeness of our approach to this reaction. The mechanism suggested here fails, however, completely for nonanalog transitions like $^{16}O(\pi^+,\pi^-)^{16}Ne$, where including more than ten intermediate ($T=1$) nuclear states in our CC system left us with a cross section more than an order of magnitude below the data.

*Also at: Institute of Nuclear Physics, Řež, Czechoslovakia.
†Also at: Department of Nuclear Physics, Charles University, CS 18000 Prague, Czechoslovakia.

[1]T.-S. H. Lee and D. Kurath, Phys. Rev. C **21**, 293 (1980).
[2]F. Lenz, M. Thies, and Y. Horikawa, Ann. Phys. (N.Y.) **140**, 266 (1982).
[3]S. Chakravarti, Phys. Lett. **90B**, 350 (1980).
[4]Z. Lleshi and R. Mach, in *Abstracts of the Contributed Papers*

of the Ninth International Conference on High Energy Physics and Nuclear Structure, Versailles, 1981, Commissariat á l'Energie Atomique ISBN 2-7272-0065-X, p. 271.
[5]D. H. Hasell *et al.*, Phys. Rev. C **27**, 482 (1983).
[6]E. Oset and D. Strottman, Nucl. Phys. **A377**, 297 (1982).
[7]E. Oset, D. Strottman, M. J. Vicente-Vacas, and Ma Wei-Hsing, Nucl. Phys. **A408**, 461 (1983).
[8]L. C. Liu, Phys. Rev. C **27**, 1611 (1983).
[9]A. K. Kerman, H. McManus, and R. Thaler, Ann. Phys. (N.Y.) **8**, 551 (1959).
[10]R. H. Landau and A. W. Thomas, Nucl. Phys. **A302**, 461 (1978).
[11]R. Mach, Czech. J. Phys. **B33**, 549 (1983); **B33**, 616 (1983).
[12]J. de Kamm, Nucl. Phys. **A360**, 297 (1981).
[13]In fact, the isobar propagation is not completely free in Eq. (2.14) because of the center-of-mass constraint used in deriving the potential matrix $U_r(E_{Ac})$.
[14]F. Lenz, Ann. Phys. (N.Y.) **95**, 348 (1975).
[15]G. A. Miller, Phys. Rev. C **10**, 1242 (1974).
[16]J. M. Eisenberg and D. Koltun, *Theory of Meson Interaction with Nuclei* (Wiley, New York, 1980).
[17]G. Rowe, M. Salamon, and R. H. Landau, Phys. Rev. C **18**, 584 (1978).
[18]J. T. Londergan, K. M. McVoy, and E. J. Moniz, Ann. Phys. (N.Y.) **78**, 299 (1973).
[19]L. Heller, G. Bohanon, and F. Tabakin, Phys. Rev. C **13**, 742 (1976).
[20]R. Mach, Nucl. Phys. **A205**, 56 (1973).
[21]M. I. Haftel and F. Tabakin, Nucl. Phys. **A158**, 1 (1970).
[22]C. M. Vincent and S. C. Phatak, Phys. Rev. C **10**, 391 (1974).
[23]A. Bohr and B. Mottelson, *Nuclear Structure* (Benjamin, New York, 1974), Vol. II.
[24]See, e.g., J. Eisenberg, Nucl. Phys. **A389**, 595 (1982).
[25]M. Gmitro, J. Kvasil, and R. Mach, Phys. Lett. **113B**, 205 (1982).
[26]C. A. Wiedner *et al.*, Phys. Lett. **78B**, 26 (1978).
[27]B. M. Preedom *et al.*, Nucl. Phys. **A326**, 385 (1979).
[28]C. A. Wiedner *et al.*, Phys. Lett. **97B**, 37 (1980).
[29]K. K. Seth, in Proceedings of the Intermediate Energy Nuclear Chemistry Workshop, Los Alamos, 1980, Northwestern University Report; S. J. Greene *et al.*, Phys. Rev. C **25**, 927 (1982).
[30]C. W. de Jager, H. de Vries, and C. de Vries, At. Data Nucl. Data Tables **14**, 479 (1974).
[31]H. Zarek *et al.*, Phys. Lett. **80B**, 26 (1978).
[32]E. W. Lees *et al.*, J. Phys. A **7**, 936 (1974).
[33]A. Nakada and Y. Torizuka, J. Phys. Soc. Jpn. **32**, 1 (1972).
[34]G. A. Miller, Nucl. Phys. **A223**, 477 (1974).
[35]P. Hoodbhoy, R. A. Freedman, G. A. Miller, and E. M. Henley, Phys. Rev. C **27**, 277 (1983); M. B. Johnson, E. R. Siciliano, H. Tobi, and A. Wirzba, Phys. Rev. Lett. **52**, 592 (1984).
[36]G. A. Miller and J. E. Spencer, Ann. Phys. (N.Y.) **100**, 562 (1976).
[37]D. A. Sparrow and A. S. Rosenthal, Phys. Rev. C **18**, 1753 (1978); X. Liu, Z. Wu, Z. Huang, and Y. Li, Sci. Sin. **24**, 789 (1981).